PHYSICAL REVIEW E **78**, 060601(R) (2008)

Understanding capillary condensation and hysteresis in porous silicon: Network effects within independent pores

Sergej Naumov, Alexey Khokhlov, Rustem Valiullin, and Jörg Kärger
Department of Interface Physics, University of Leipzig, D-04103 Leipzig, Germany

Peter A. Monson
Department of Chemical Engineering, University of Massachusetts, Amherst, Massachusetts 01003, USA
(Received 8 August 2008; published 1 December 2008)

The ability to exert a significant degree of pore structure control in porous silicon materials has made them attractive materials for the experimental investigation of the relationship between pore structure, capillary condensation, and hysteresis phenomena. Using both experimental measurements and a lattice gas model in mean field theory, we have investigated the role of pore size inhomogeneities and surface roughness on capillary condensation of N_2 at 77 K in porous silicon with linear pores. Our results resolve some puzzling features of earlier experimental work. We find that this material has more in common with disordered materials such as Vycor glass than the idealized smooth-walled cylindrical pores discussed in the classical adsorption literature. We provide strong evidence that this behavior comes from the complexity of the processes within independent linear pores, arising from the pore size inhomogeneities along the pore axis, rather than from cooperative effects between different pores.

DOI: 10.1103/PhysRevE.78.060601 PACS number(s): 68.03.Fg, 05.70.Np, 64.60.My, 68.43.Mn

The reduced dimensionality of nanocrystalline Si results in its very interesting properties with a wealth of potential applications, especially in photonics [1–3]. Electrochemical etching of bulk Si provides an extremely simple approach to form porous silicon (PSi), a material composed of a nanocrystalline skeleton enclosed in a network of pores. In this sense, PSi is sometimes referred to as *quantum sponge* where effects of quantum confinement play a fundamental role [2]. Among the various features, brought about by the procedure of PSi nanostructuring, it is in particular the intrinsic mesoscale disorder that plays a crucial role in determining the material properties. Some prominent examples are disorder-induced localization of electronic states, anomalous carrier transport, slow conductivity, and aging [4,5]. Since, simultaneously, it is this disorder that severely limits the technological application of PSi, deeper insight into its nature and the consequences of its occurrence is urgently needed.

Remarkably, exploration of disorder in PSi has also been in the focus of a second scientific community concerned with the properties of condensed phases confined in the pores of PSi. The option to produce PSi's with tailor-made pores of varying diameters and constrictions has made them ideal model systems for investigations of the relationship between pore structure, capillary condensation, and hysteresis phenomena [6–10].

The earliest studies on capillary condensation in PSi with linear pores [6,7] revealed two striking features: the adsorption and desorption branches of the hysteresis loop were not parallel, as would be expected for a distribution of independent pores [11], and the hysteresis was unchanged upon closing the pores at one end. Closing the end of idealized smooth-walled independent pores is expected to eliminate hysteresis since the pore end promotes condensation, as was suggested in the classical work of Cohan [12] and confirmed by computer simulation studies [13]. The results obtained in these early studies [6,7] called into question the applicability of the Cohan analysis and the tentative conclusion was made that the pores in these systems do not behave independently with respect to adsorption and desorption due to long-range interactions between pores [9].

Knorr and co-workers [8] were able to investigate inkbottlelike geometries by studying PSi with two different segment diameters of about $d_s \approx 5$ nm and $d_l \approx 6$ nm within the same pore channel. From their observations they concluded that the effects of this geometry are submerged by the overall surface roughness. They concluded that the pores can be regarded as chains of pore segments with a distribution of diameters, creating quenched disorder along the length of the pore. The most puzzling feature of their analysis was that this roughness, namely, random variation of the pore diameter along the pores, would be expected to be smaller than the difference $d_l - d_s$, while being sufficient to eliminate typical effects of inkbottle geometry, such as cavitation or pore blocking, as extensively discussed in the literature [13,14]. The physical origin of such behavior is uncertain. Indeed, in Ref. [9] similar experimental evidence has been attributed to the influence of interactions between the pores.

To clarify the issues emerging from previous work, we have performed a series of investigations including (i) obtaining direct experimental evidence that for the PSi under study any interaction between adjacent channel pores due to intersections may be safely excluded, (ii) the reproduction of the hysteresis pattern (N_2 in PSi; 77 K) with asymmetric adsorption and desorption branches, including evidence of divergence in the relaxation times in the hysteresis region, (iii) the application of mean field theory of a lattice gas for quantifying the effect of disorder on the state of the intrapore fluid and, as an immediate outcome of the calculations, and (iv) visualizations of the fluid density distributions for states traversed on the hysteresis loop.

PSi was prepared by electrochemical etching of a B-doped (100) silicon wafer in HF solution, taking particular

care to ascertain that there are no intersections between neighboring pores. This could be achieved by the proper matching of doping level, HF concentration, and etching current density j [7,15]. We found that, for the substrate with a resistivity of 2–5 mΩ cm used, the optimal conditions corresponded to etching using 48% aqueous HF solution mixed in equal volumes with ethanol and by applying $j=20$ mA/cm^2. Two types of sample were used for further experiments: one with the porous film detached from the substrate (pores open at both ends) and the other with the porous film on the substrate (pores open at only one end). In both cases, the film thickness was 30 μm.

We used pulsed field gradient nuclear magnetic resonance (PFG NMR) to probe for any effects of interconnections (and, hence, of an undesired interaction) between the different pore channels. As a probe of the spatial anisotropy of molecular propagation [16,17], PFG NMR is able to yield simultaneously the molecular diffusivities along the pores, $D_\parallel$, and in the radial direction, $D_\perp$. In the absence of interconnections, the latter should vanish. PFG NMR is based on the creation of a magnetic field gradient, leading to position-dependent resonance frequencies ω of the nuclear spins. Application of a pair of such pulses with opposite directions, separated by an evolution time t, allows assessment of the displacements of spin-bearing molecules by measurement of a mismatch in ω at these two instants of time. If the applied gradients are linear in space, this mismatch is ultimately proportional to the projection of the displacement onto this axis. As a result, the measured NMR signal intensity S for a powdered material can be shown to be [16]

$$S \sim \int_0^{2\pi} \exp\{-[D_\parallel \cos^2(\Omega) + D_\perp \sin^2(\Omega)]q^2 t\}\sin(\Omega)d\Omega, \tag{1}$$

where q is the wave number, controlled by the experimental conditions, and Ω is the angle between the pore axes and the direction along which the displacements are registered, namely, the direction of the magnetic field gradient.

Figure 1 shows the PFG NMR signal measured in a powder sample of PSi by means of a 13-interval pulse sequence [18]. As a probe liquid, *n*-eicosane was used. Its sufficiently low vapor pressure ensured that there was no contribution of interpore hopping through the vapor phase at the pore ends. Notably, the shape of $S(q)$ is well captured by Eq. (1), with $D_\parallel = 2.6\times10^{-11}$ m^2/s and $D_\parallel/D_\perp > 10^4$. With the chosen observation time of $t=80$ ms, displacements of 2 μm in the channel direction are found to be accompanied, if at all, by displacements perpendicular to this direction of less than 20 nm. Hence, any notable contact between the pore volumes of adjacent channels may be excluded. For comparison, Fig. 1 also includes the experimental data (squares) for an analogous measurement where the PSi was produced by an etching current of $j=76$ mA/cm^2 (rather than 20 mA/cm^2). Now the respective diffusivities are $D_\parallel = 1.4\times10^{-10}$ m^2/s and $D_\perp = 2.8\times10^{-12}$ m^2/s. This means that, during a displacement of 5 μm in the channel direction, the probe molecules would undergo a shift of about 0.7 μm perpendicular to it, reflecting substantial damage in the walls between adjacent channel pores.

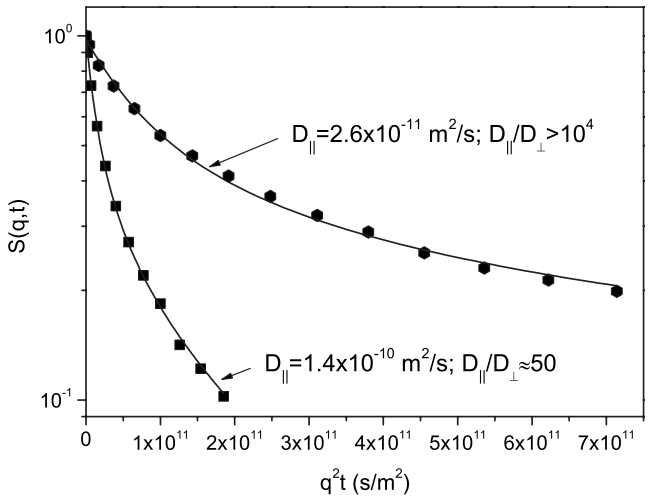

FIG. 1. Primary data $S(q)$ for the PFG NMR diffusion measurement of probe molecules (*n*-eicosan at room temperature) in the PSi sample used in this study (circles) and in a second PSi sample (squares). In the latter case, the etching current was intentionally chosen notably larger to generate interconnections between adjacent channel pores. The measurements have been performed with powder samples. While within the PSi sample used in the present study diffusion is found to be essentially one dimensional ($D_\parallel/D_\perp > 10^4$), a value of $D_\parallel/D_\perp \approx 50$ as resulting from curve analysis of the second sample reveals notable damage of the channel walls.

Experimental volumetric sorption isotherms for N_2 at 77 K are shown in Fig. 2. In common with the earlier studies [6–9], we find hysteresis loops where the adsorption and desorption branches are not parallel and which remain unaffected by opening and closing one end of the pore. The inset of Fig. 2 illustrates the process of relaxation toward different,

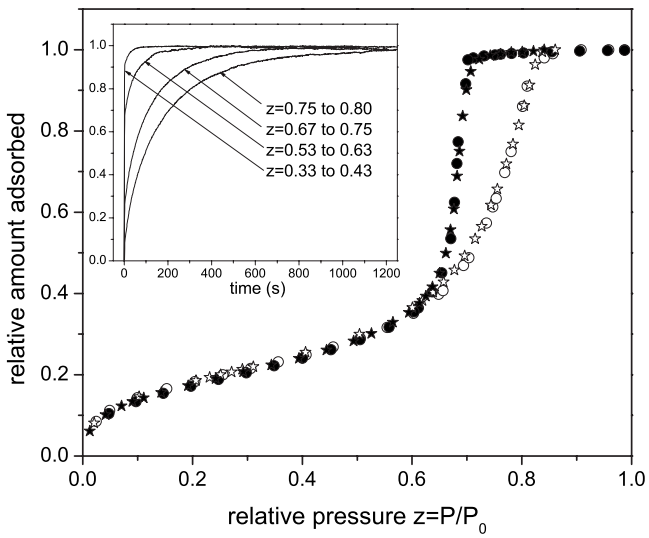

FIG. 2. Relative adsorption (open symbols) and desorption (filled symbols) for liquid nitrogen in porous silicon open at both ends (circles) and at one end (stars). The inset shows adsorption transients upon a stepwise change of the external vapor pressure as indicated in the figure.

individual states on the adsorption branch of the isotherm. It is expressed by the relative uptake following a small stepwise change of the external vapor pressure. It is evident that the relaxation becomes very slow as the system enters the hysteresis region. Following the analysis of Ref. [19], this slowing down cannot be related to a change of the diffusive properties of the adsorbed molecules. Rather, it is due to a much slower process of density evolution in the pores.

Both the dynamics and the sorption isotherms suggest that PSi exhibits the effects of quenched disorder, completely consistent with our earlier work on adsorption in Vycor random porous glass [19,20]. Here, the underlying physics in the hysteresis is dominated by the appearance of many metastable states (local minima of the grand free energy of the system) arising from the very large number of ways of distributing the fluid inside the porous material for a given average density along the pore. The very slow dynamics arises from the need to cross the free energy barriers between these states in the relaxation to equilibrium. The shape of the adsorption isotherm and the metastable states in the hysteresis region are well described qualitatively via mean field theory for a lattice gas model [20,21]. We are going to show that, without any need for additional mechanisms, this same approach is also able to correlate the local disorder of PSi channel pores with the macroscopically observable effects of hysteresis.

Our model of the fluid in the pore is similar to that used in recent studies [20,21] and uses a cubic lattice with nearest neighbor interactions. We write the grand free energy in mean field theory as

$$\Omega = kT\sum_{\mathbf{i}} [\rho_{\mathbf{i}} \ln \rho_{\mathbf{i}} + (1-\rho_{\mathbf{i}})\ln(1-\rho_{\mathbf{i}})] - \frac{\epsilon}{2}\sum_{\mathbf{i}}\sum_{\mathbf{a}} \rho_{\mathbf{i}}\rho_{\mathbf{i}+\mathbf{a}} + \sum_{\mathbf{i}} \rho_{\mathbf{i}}[\phi_{\mathbf{i}} - \mu]. \quad (2)$$

Here ϵ is the nearest neighbor interaction strength, $\rho_{\mathbf{i}}$ is the average occupancy at site $\mathbf{i}$, $\phi_{\mathbf{i}}$ is the external field at site $\mathbf{i}$, with $\mathbf{i}$ denoting a set of lattice coordinates, and $\mathbf{a}$ denotes the vector to a nearest neighbor site. $\phi_{\mathbf{i}}$ is also modeled as a nearest neighbor interaction (between fluid occupied sites and sites in the pore wall) but with strength 2ϵ. The necessary condition for a minimum in the grand free energy leads to a set of nonlinear algebraic equations that can be solved to obtain the density distribution $\{\rho_{\mathbf{i}}\}$. The geometry we considered consists of a slit pore that is open to the bulk on two opposite ends while infinite in the other direction. This geometry has similar behavior to that of a cylindrical pore (as can be seen by comparing the results in Ref. [22] for cylindrical pores with those in Ref. [13] for slit pores) but the problem can be rendered two dimensional with a considerable saving in computer time for long pores. We divided the pore into 100 segments, each of length 10 lattice constants. Each of these segments has a diameter chosen randomly in the range 4–8 lattice constants from a discrete Gaussian distribution with a mean diameter of 6 lattice constants. We averaged the properties from mean field calculations over 50 realizations of the pore. The model pore geometry is qualitatively consistent with the earlier suggestion about the nature of the quenched disorder in PSi [8], although the variation in pore diameter used in our calculations is somewhat larger than that anticipated in that work. In addition, we modeled small-scale disorder by randomly adding single solid sites to the pore surface that also interact with the fluid sites via $\phi_{\mathbf{i}}$, while removing solid sites from other points on the surface to preserve the porosity. We chose a temperature $kT/\epsilon = 1$ (kT is Boltzmann's constant times the absolute temperature), which is 2/3 of the bulk critical temperature for the simple cubic lattice gas in mean field theory. Nitrogen at 77 K is at about 61% of its bulk critical temperature.

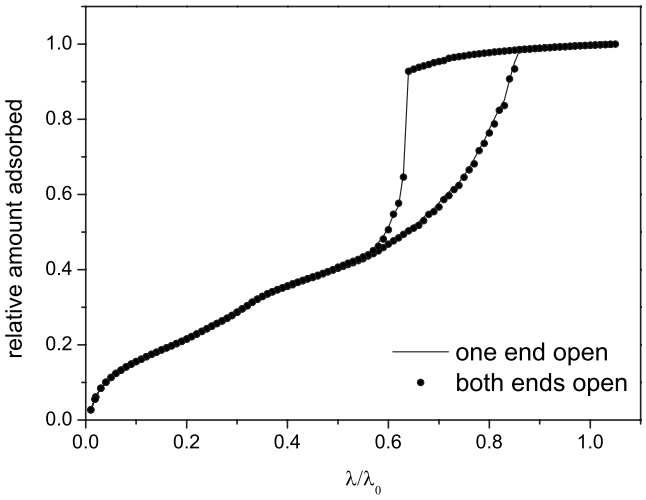

FIG. 3. Theoretical sorption isotherms calculated using mean field theory of a lattice gas model for a model of linear pores with superimposed disorder. The density is plotted vs the bulk relative activity λ/λ_0, where $\lambda = \exp(\mu/kT)$ is the activity, with μ the chemical potential; the 0 subscript refers to the bulk saturation state. The relative activity is close to the relative pressure except for the small effects of bulk gas imperfection.

Figure 3 presents the sorption isotherms for the model with both open-ended pores and pores with one end closed. The model correctly reproduces the shape of the experimental sorption isotherms for N_2 in PSi. Moreover, the results for pores closed at one end are identical to those for a pore open at both ends.

Visualizations of the density distributions for states along the isotherms are shown in Fig. 4 for one realization of the pore open at both ends—closing one end of the pore does not change the picture (for these visualizations we use a pore with 50 segments). At low activities the isotherm is associated with the covering of the pore walls with adsorbed layers. Importantly, the small-scale surface roughness is only of importance in determining the proper isotherm curvature before onset of hysteresis by, e.g., smearing out signatures of the two-dimensional surface condensation transition. At intermediate activities we see condensation of liquid bridges where the pore width is smallest. For the closed pore these condensations may have already occurred before pore condensation is under way at the closed end. This explains why Cohan's analysis [12], which applies to an idealized smooth-walled pore, is not applicable here [7]. At higher activities we have condensation of liquid bridges in regions of higher pore diameter as well as growth of liquid bridges condensed

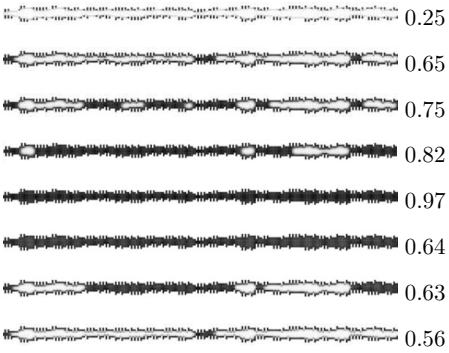

FIG. 4. Visualizations of the density distribution from mean field theory for a single realization of a 50-segment pore. The states are, from top to bottom, λ/λ_0=0.25, 0.65, 0.75, 0.82, and 0.97 on adsorption followed by λ/λ_0=0.64, 0.63, and 0.56 on desorption. Darker shading corresponds to regions of higher density. Only one-half of the pore is shown with the pore opening on the left.

at lower activity. Through these processes the system progressively fills with liquid.

On desorption, the model predicts first a loss of density leading to an expanded liquid throughout the pore. Further decrease of the gas pressure leads to a more significant loss of density through a combination of cavitation [13,14] and evaporation from liquid menisci (delayed by pore blocking). Importantly, as a consequence of strong disorder, the very first cavities may occur in the pore body far away from the pore ends. This may help to rationalize puzzling desorption behavior from the inkbottle systems observed in Ref. [8]. Irrespective of whether the bottle part has direct contact to the bulk phase or not, desorption is initiated by cavities formed in the pore body. Thus, isotherms for the two inkbottlelike configurations in Ref. [8] become largely indistinguishable.

In summary, our experiments and theoretical calculations have identified the effects of quenched disorder in the channel pores of PSi as the directing feature for adsorption hysteresis. Importantly, our calculations suggest that this disorder has to be relatively pronounced, exceeding disorder on an atomistic level. Thus, the channel pores of PSi turn out to exhibit all effects more commonly associated with three-dimensional disordered networks. In addition, however, their simple geometry makes them an ideal model system for experimental observation and theoretical analysis.

This work was supported at the University of Leipzig by DFG and at the University of Massachusetts by the NSF Grant No. CBET-0649552.

[1] A. G. Cullis, L. T. Canham, and P. D. J. Calcott, J. Appl. Phys. **82**, 909 (1997).
[2] O. Bisi, S. Ossicini, and L. Pavesi, Surf. Sci. Rep. **38**, 1 (2000).
[3] D. Kovalev and M. Fujii, Adv. Mater. (Weinheim, Ger.) **17**, 2531 (2005).
[4] M. V. Wolkin, J. Jorne, P. M. Fauchet, G. Allan, and C. Delerue, Phys. Rev. Lett. **82**, 197 (1999).
[5] S. Borini, L. Boarino, and G. Amato, Phys. Rev. B **75**, 165205 (2007).
[6] B. Coasne, A. Grosman, N. Dupont-Pavlovsky, C. Ortega, and M. Simon, Phys. Chem. Chem. Phys. **3**, 1196 (2001).
[7] B. Coasne, A. Grosman, C. Ortega, and M. Simon, Phys. Rev. Lett. **88**, 256102 (2002).
[8] D. Wallacher, N. Kunzner, D. Kovalev, N. Knorr, and K. Knorr, Phys. Rev. Lett. **92**, 195704 (2004).
[9] A. Grosman and C. Ortega, Langmuir **24**, 3977 (2008).
[10] S. Gruener and P. Huber, Phys. Rev. Lett. **100**, 064502 (2008).
[11] K. S. W. Sing, D. H. Everett, R. A. W. Haul, L. Moscou, R. A. Pierotti, J. Rouqerol, and T. Siemieniewska, Pure Appl. Chem. **57**, 603 (1985).
[12] L. H. Cohan, J. Am. Chem. Soc. **60**, 433 (1938).
[13] L. Sarkisov and P. A. Monson, Langmuir **17**, 7600 (2001).
[14] P. Ravikovitch and A. Neimark, Langmuir **18**, 9830 (2002).
[15] V. Lehmann, R. Stengl, and A. Luigart, Mater. Sci. Eng., B **69**, 11 (2000).
[16] P. T. Callaghan, *Principles of Nuclear Magnetic Resonance Microscopy* (Clarendon Press, Oxford, 1991).
[17] K. Hahn, J. Kärger, and V. Kukla, Phys. Rev. Lett. **76**, 2762 (1996).
[18] R. M. Cotts, M. J. R. Hoch, T. Sun, and J. T. Markert, J. Magn. Reson. (1969-1992) **83**, 252 (1989).
[19] R. Valiullin, S. Naumov, P. Galvosas, J. Kärger, H.-J. Woo, F. Porcheron, and P. A. Monson, Nature (London) **443**, 965 (2006).
[20] H.-J. Woo and P. A. Monson, Phys. Rev. E **67**, 041207 (2003).
[21] E. Kierlik, P. A. Monson, M. L. Rosinberg, L. Sarkisov, and G. Tarjus, Phys. Rev. Lett. **87**, 055701 (2001).
[22] L. D. Gelb, Mol. Phys. **100**, 2049 (2002).